ELSEVIER

Catalysis Today 58 (2000) 335–344

CATALYSIS TODAY

www.elsevier.com/locate/cattod

Development of Fe Fischer–Tropsch catalysts for slurry bubble column reactors

K. Jothimurugesan[a,*], James G. Goodwin[b] Jr., Santosh K. Gangwal[c], James J. Spivey[c]

[a] *Department of Chemical Engineering, Hampton University, Hampton, VA 23668, USA*
[b] *Department of Chemical and Petroleum Engineering, University of Pittsburgh, Pittsburgh, PA 15260, USA*
[c] *Research Triangle Institute, PO Box 12194, Research Triangle Park, NC 27709, USA*

Abstract

The effect of two binder systems — a silica-based system and a silica–kaolin–clay–phosphate-based system — on a doubly promoted Fischer–Tropsch (FT) synthesis iron catalyst (100Fe/5Cu/4.2K) was studied. The catalysts were prepared by coprecipitation, followed by binder addition and spray drying at 270°C in a 1 m diameter, 2 m tall spray dryer. The binder silica content was varied from 0 to 20 wt.%. A catalyst with 12 wt.% binder silica was found to have the highest attrition resistance. The FT activity and selectivity of this catalyst are better than a Ruhrchemie catalyst at 270°C and 1.48 MPa. The addition of precipitated silica or kaolin to catalysts containing 10–12 wt.% binder silica decreases attrition resistance and increases methane selectivity. Based on the experience gained, a catalyst has been successfully spray dried in 500 g quantity. This catalyst showed 95% CO conversion over 125 h of testing at 270°C, 1.48 MPa, and 2 NL/g-cat/h and had less than 4% methane selectivity. Its attrition resistance was one of the highest among the catalysts tested.

Keywords: Fischer–Tropsch synthesis; Iron catalysts; Carbon monoxide hydrogenation; Attrition; Slurry bubble column reactor

1. Introduction

Fischer–Tropsch synthesis (FTS) to convert syngas ($CO+H_2$) derived from natural gas or coal to liquid fuels and wax is a well-established technology. For low H_2/CO ratio syngas produced from CO_2 reforming of natural gas or from gasification of coal, the use of Fe catalysts is attractive because of their high water gas shift activity in addition to their high FT activity. Fe catalysts are also attractive because of their low cost and low methane selectivity [1–3]. Because of the highly exothermic nature of the FT reaction, there has been a recent move away from fixed-bed reactors toward the development of slurry bubble column reactors (SBCRs) that employ 30–90 μm catalyst particles suspended in a waxy liquid for efficient heat removal [4–5].

Although much recent work related to slurry-phase FTS based on coal-derived syngas has focused on Fe catalysts, the use of Fe catalysts in SBCRs has faced a number of problems. Because of the difficulty in reducing highly dispersed supported Fe, and the lower FTS activity of Fe compared to Co or Ru, bulk Fe catalysts must be used in order to have sufficient active surface area per catalyst weight. The Fe catalysts used in SBCRs have typically been prepared by precipitation, which is the usual method of preparing of Fe catalysts for fixed-bed reactors.

The problems encountered in using precipitated iron catalysts are mainly due to two major properties: their

* Corresponding author.

0920-5861/00/$ – see front matter
PII: S0920-5861(00)00266-2

low density and their poor attrition resistance. Low density leads to difficulties in separating the catalyst from the reaction mixtures. Because SBCRs are used to produce high molecular weight (high alpha; α) FTS products, there is a need to easily and inexpensively separate the catalyst from these liquid products. The apparent density of typical precipitated Fe catalysts (near 0.7 g/cm^3) is close to that of Fischer–Tropsch wax (about 0.68 g/cm^3) at reaction conditions [6]. Although this helps to keep the catalyst suspended in the slurry, catalyst separation from the products can be difficult since the catalyst does not settle well. Although internal/external filtration systems can be incorporated with slurry reactors, plugging of the filters by Fe catalyst particles is often encountered. This is due to the low attrition resistance of the Fe catalyst and the significant breakage of the Fe particles [7].

Fe catalysts are subject to both chemical and physical attrition in a SBCR. Chemical attrition can be caused by phase changes that affect all Fe catalysts ($Fe_2O_3 \rightarrow Fe_3O_4 \rightarrow FeO \rightarrow$ Fe metal $\rightarrow$ Fe carbides), potentially causing internal stresses within the particle and resulting in weakening, spalling or cracking [8,9]. Physical attrition can result from collisions between catalyst particles and the reactor wall. Catalyst particles of irregular shapes and non-uniform sizes produced by conventional methods are subject to greater physical attrition.

The objective of this study is to develop attrition-resistant Fe FT catalysts suitable for SBCR applications. Binders are necessary to impart attrition resistance to the catalyst particles. However, improvement in attrition resistance at the expense of activity and selectivity is undesirable. In this study the effect of two binder systems — a silica-based system and a silica–kaolin–clay–phosphate-based system — on activity, selectivity, and attrition resistance of precipitated Fe FT catalysts is evaluated.

2. Experimental

2.1. Catalysts preparation

A standard Ruhrchemie precipitated Fe catalyst (identified as batch 52119) was obtained from the US Department of Energy (DOE) as a benchmark catalyst. The composition of this catalyst was 100Fe/5Cu/4.2K/25SiO_2. It contained 25 parts by weight (pbw) of precipitated silica. It was obtained as a 1/8 in. extrudate and was crushed from 50 to 100 μm particles prior to use. This catalyst served as a basis of comparison for the activity, but not attrition resistance, of the catalysts synthesized in the work presented here.

A cobalt catalyst with 20 wt.% of cobalt, prepared using incipient wetness of spray dried silica (Davison Grade 952), was also used as a benchmark. This cobalt catalyst was found to be suitable for use in SBCR [10]. This cobalt catalyst will serve as a baseline catalyst for this work, from which improvements in attrition will be sought.

In this study, all catalysts were prepared with the same ratio of iron, copper, and potassium (100Fe/5Cu/4.2K) as the benchmark, but with differing levels and types of binder and differing levels of precipitated silica. Four types of catalysts were prepared as shown in Table 1. Catalyst preparation involved four steps: preparation of the iron, copper, and silica (when added) precursor; incorporation of potassium; addition of binder silica and kaolin–phosphate binder; and spray drying. The constant pH precipitation technique used to prepare the Fe/Cu/Si catalyst precursor has been described in detail previously [11]. In brief, the catalyst precursor was continuously precipitated from flowing aqueous solution containing iron nitrate, copper nitrate, and (when added) tetraethylorthosilicate at the desired Fe/Cu/Si ratio using aqueous ammonia. The precipitate was then thoroughly washed with deionized water by vacuum filtration. The potassium promoter was added as aqueous potassium bicarbonate solution to the undried, reslurried Fe/Cu/Si coprecipitate.

The binder silica preparation and addition method is the subject of a patent application and is not disclosed here. The kaolin binder was prepared by diluting kaolin with distilled water following the procedure described by Demmel [12]. To the diluted kaolin, 85 wt.% phosphoric acid was added, followed by 40 wt.% dibasic ammonium phosphate to bring the pH to 7. The Fe/Cu/K/Si slurry was added to the clay slurry and mixed in a blender. The slurry was spray dried in a large bench-scale Niro spray drier of 3 ft diameter and 6 ft height. Finally, the spray dried catalyst was calcined at 300°C for 5 h in a muffle furnace.

Table 1
Catalyst designation and binder content

Catalyst	Series binder silica (wt.%)	Precipitated silica (pbw)	Kaolin binder (wt.%)
Fe–bSi(*x*)	*x*	0	0
Fe–pSi(*y*)	12	*y*	0
Fe–KL(*z*)	10	0	*z*
Ruhrcheime HPR	0	25 Proprietary composition	0

2.2. Catalyst characterization

Detailed physical and chemical characterization of the fresh, reduced, and used catalysts was carried out using the following analytical techniques. The BET surface area of the catalysts was determined by N_2 physisorption using a Micromeritics Gemini 2360 system. The samples were degassed in a Micromeritics Flow Prep 060 at 120°C for 1 h prior to each measurement. The SEM micrograph was taken using a Cambridge Stereoscan 100. X-ray powder diffraction patterns were obtained using a Phillips PW1800 X-ray unit using Cu Kα radiation. Analyses were conducted using a continuous scan mode at a scan rate of 0.05° 2θ per second.

For determination of the reduction behavior and the reducibility of the catalysts, TPR experiments were carried out using a Micromeritics 2705 TPR/TPD system. A sample close to 0.2 g was dried and degassed under high purity Ar at 400°C for 1 h, and this was followed by cooling the sample to ambient temperature. Reduction was achieved under H_2/Ar gas mixture (volume ratio 5/95). The total gas flow was 40 cm^3/min, and temperature program was 25–900°C at a heating rate of 10°C/min. Hydrogen consumed by the catalyst was detected using a thermal conductivity detector (TCD) and recorded as a function of temperature.

The attrition of the catalysts was measured using test method ASTM-D-5757-95 in a three-hole air-jet attrition tester. This test method is applicable to spherically or irregularly shaped particles that range in size between 10 and 180 μm, have skeletal densities between 2.4 and 3.0 g/cm^3, and are insoluble in water. Particles less than 20 μm are considered fines. The system consists of a vertical attrition tube, a stainless steel tube 710 mm long with an inside diameter of 35 mm. There is an orifice plate attached to the bottom of this tube with three 2 mm long drilled sapphire square-edged nozzles. The nozzles are precision drilled and are 0.381+/−0.005 mm in diameter. Above the attrition tube is the settling chamber, a 300 mm long cylinder with a 110 mm inside diameter. Finally, there is a fines collection assembly composed of a 250 ml filtering flask and an extraction thimble. There is additional peripheral equipment required to provide the source of humidified air (30–40% relative humidity) that the test method requires. To conduct a test, a sample of dried powder is humidified and subjected to attrition by means of three high velocity jets of humidified air. The fines are continuously removed from the attrition zone by elutriation into a fines collection assembly. The attrition loss is calculated from the elutriated fines to give a relative estimate of the attrition resistance of the powdered catalyst. The full test protocol calls for 45 g of a screened and dried representative sample to be humidified with 5 g of demineralized water to produce 50 g of water equilibrated sample. This sample is run in the apparatus for 5 h, with an intermediate change of the fines filter at 1 h elapsed time. The attrition loss is based on the fines loss after 1 and 5 h.

2.3. Reaction studies

The catalysts prepared were tested in a laboratory-scale high-pressure and high-temperature fixed-bed reactor, which is shown in Fig. 1. The fixed-bed reactor was constructed of a 1 cm i.d. stainless steel tube. The iron FT catalysts were pretreated under flowing CO at 280°C for 16 h before reaction. Following catalyst pretreatment, the reactor temperature was decreased to 50°C. CO flow was stopped, and synthesis gas flow was begun at a gas space velocity of 2.0 NL/g-cat/h. The synthesis gas was a premixed gas of CO and

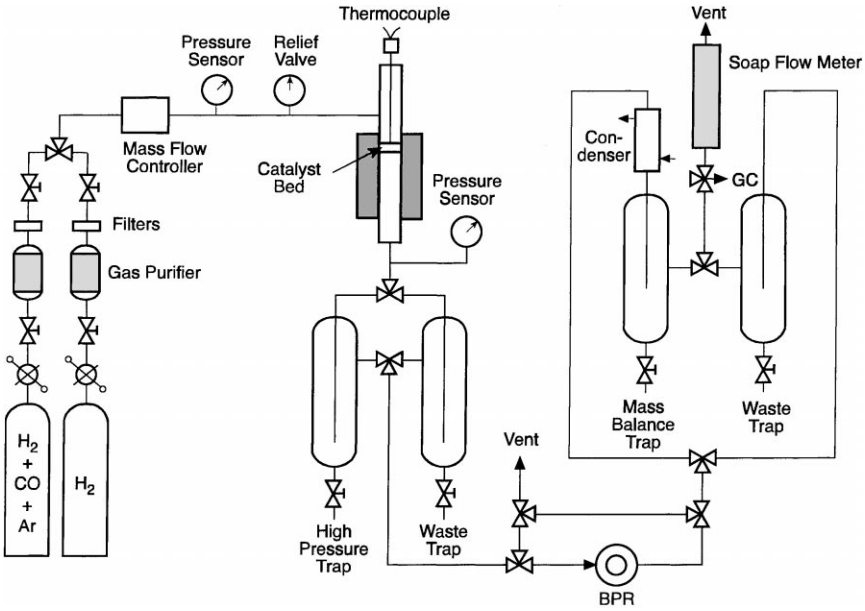

Fig. 1. Schematic diagram of the laboratory-scale fixed-bed reactor.

H_2 (H_2/CO=0.67) containing 5% Ar as an internal standard for use in product analysis. The reactor system was then pressurized to 1.48 MPa, and the reactor temperature was increased gradually to 270°C. This is referred to as the conditioning period. After achieving the desired process condition of 270°C, 1.48 MPa, 2.0 NL/g-cat/h, and H_2/CO=0.67, the catalyst was tested over a period of 80–125 h.

The product gas was analyzed by an online Hewlett-Packard (HP) 5890 gas chromatograph (GC), with advanced Chemstation control. Three valves were used in the system: a 6-port gas sampling valve, a 10-port gas sampling valve with backflush to vent, and a 6-port column isolation valve. The hydrocarbons C_1–C_{15} and the oxygenates were analyzed using an HP-1 100 m × 0.25 mm × 0.5 μm capillary column and detected by a flame ionization detector (FID). The CO, CO_2, and Ar were separated by a 2.6 ft × 1/8 in. Haysep Q column and 3.15 ft × 1/8 in. molecular sieve 13× columns, and were detected by TCD. The wax samples were analyzed using a SPB-1 15 m × 0.53 m × 0.1 μm capillary column with an FID. The calibration was carried out using various calibration mixtures and pure compounds from Supelco and HP.

3. Results and discussion

Fig. 2 illustrates the morphologies of binder silica, precipitated silica and kaolin–clay catalysts. Catalysts are roughly spherical in shape, typical of a spray drying process, with diameters ranging from 30 to 90 μm.

Table 2 shows the BET surface areas of the fresh and reduced catalysts, the hydrogen uptake, pore volume, and attrition properties of all the catalysts synthesized. The attrition resistance of the binder silica-based catalysts (with no precipitated silica) increased (i.e., attrition is reduced) as binder level was increased up to 12 wt.%, then decreased when the binder level was increased to 20 wt.%, indicating an optimum binder silica level of about 10–12 wt.%. The Fe–pSi series containing precipitated silica was prepared with 12 wt.% binder silica. As the precipitated silica content increased from 5 to 20 parts by weight, the attrition became so severe that it plugged the attrition tester during a 5 h test. Data from a cobalt catalyst with 20 wt.% cobalt prepared using incipient wetness of a spray dried silica is also listed in Table 2 as a benchmark. This cobalt catalyst was found to be suitable for use in a SBCR [10]. The comparison of the attrition results shows that some of the spray dried

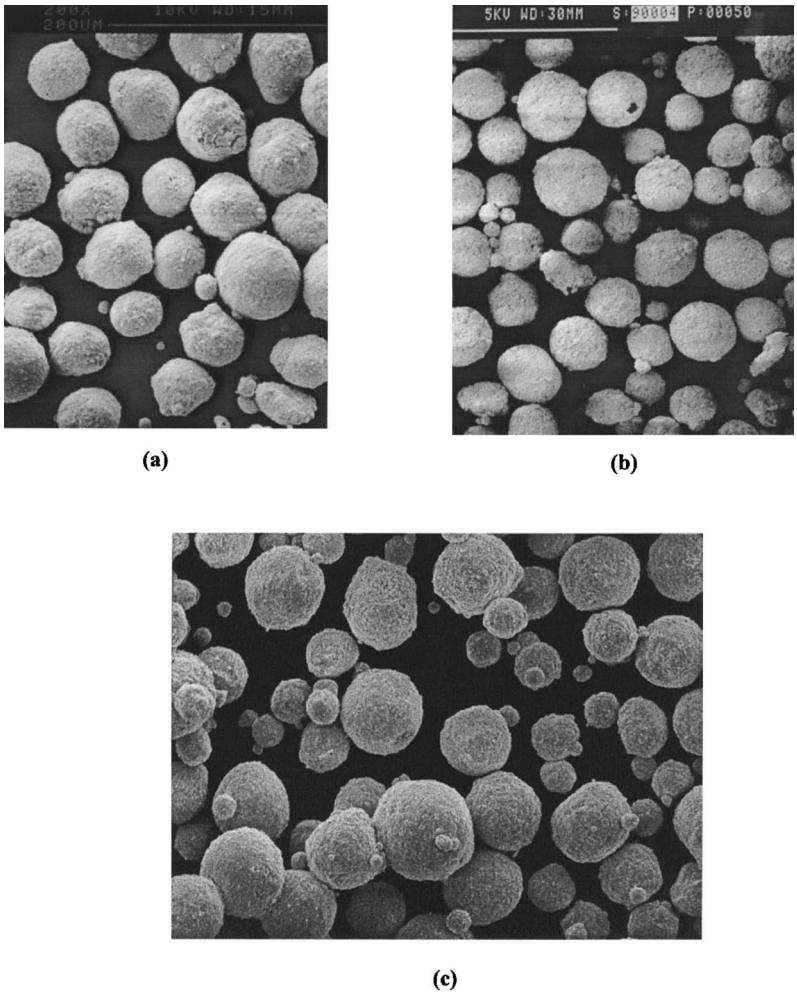

Fig. 2. SEM image of the spray dried precipitated iron catalysts: (a) FE–bSi(12); (b) Fe–pSi(15); and (c) Fe–KL(12).

iron catalysts in their calcined state are physically as strong as, or stronger than, the cobalt catalyst. These iron catalysts are therefore candidates for SBCR use.

The Fe–KL series containing kaolin binder was prepared with 10 wt.% binder silica. As with precipitated silica, increase of the kaolin content from 8 to 24 wt.% increased the attrition loss. However, there was one difference in the trend of increase between the two additives. In the case of precipitated silica addition, the 1 h attrition increased significantly, whereas in the case of kaolin addition, the 5 h attrition increased significantly. This seems to indicate the formation of a greater number of fines ($<20\,\mu m$) with precipitated silica during preparation. These fines are removed during the first hour. On the other hand, with kaolin binder, although fines do not increase significantly with the binder content, the larger catalyst particles break apart significantly between 1 and 5 h, resulting in fines.

Although the catalysts were prepared under similar conditions using the spray drying technique, the attrition resistances vary over a large range (Table 2). After the addition of both precipitated silica and kaolin, not only is the overall catalyst attrition worse than that of the catalysts containing only binder silica, but

Table 2
Physical and chemical properties of Fe catalysts

Catalyst designation	BET surface area (m^2/g)		TPR measurements (H_2 consumed, mmol/g-cat)	Attrition loss (wt.%)		Pore volume (cm^3/g)
	Fresh	Reduced		1 h	5 h	
Fe–bSi(4)	80.3	35.6	24.3	24.4	32.6	0.58
Fe–bSi(8)	95.7	50.8	23	25.7	35.4	0.56
Fe–bSi(12)	121	68.7	20.6	12.8	22.7	0.56
Fe–bSi(16)	151	103	19	22.0	30.1	0.68
Fe–bSi(20)	172	98.9	18.4	34.9	35.0	0.68
Fe–pSi(5)	163	116	18.8	24.2	37.3	0.54
Fe–pSi(10)	168	144	17.9	31.0	39.6	0.54
Fe–pSi(15)	189	163	17.7	42.1	[a]	0.62
Fe–pSi(20)	218	181	17.6	39.1	[a]	0.64
Fe–KL(8)	195	NM[b]	22.8	8.8	27.9	NM
Fe–KL(12)	190	NM	21.5	17.3	56.8	NM
Fe–KL(16)	191	NM	21.6	8.4	27.6	NM
Fe–KL(20)	192	NM	21.1	19.9	44.0	NM
Fe–KL(24)	193	NM	22.5	17.9	54.1	NM
HPR-39	107.8	NM	NM	4.7	10.0	NM
HPR-40	81.4	NM	NM	4.1	9.7	NM
HPR-41	60.5	NM	NM	6.4	17.7	NM
HPR-42	79.8	NM	NM	5.2	15.5	NM
HPR-43	81.5	NM	NM	7.6	14.6	NM
Ruhrchemie	300	NM	NM	NM	NM	NM
Co/SiO_2	NM	NM	NM	31.07	NM	NM

[a] Tester plugged due to severe attrition.
[b] NM=not measured.

the attrition resistance also decreases with an increasing levels of precipitated silica and kaolin. The result found here with kaolin is in agreement with data from the literature [13]. The optimum non-proprietary catalyst with respect to attrition is the one with binder silica at a 10–12 wt.% level and no precipitated silica or kaolin.

A series of catalysts designated HPR was prepared to further improve attrition resistance. The binder silica for these catalysts was identical to that used for the Fe–bSi catalysts; however, the method of binder addition was changed. (This novel method is not disclosed here because of a pending patent.) As can be seen in Table 2, these catalysts have significantly improved attrition resistance, even better than the Fe–bSi series of catalysts. Finally, an HPR-43 material (which is a nominal duplicate of HPR-40) was prepared a larger 500 g batch to evaluate scalability of the preparation technique. As can be seen, the larger batch had a somewhat higher attrition than HPR-40, but still had significantly lower attrition than the Fe–bSi series of catalysts.

As shown in Table 2, the BET surface area of the catalysts increased with an increase in concentration of both binder silica and precipitated silica. The series with precipitated silica had relatively higher surface areas compared with the series with binder silica. However, there appears to be no effect on surface area as the content of the kaolin binder increased from 8 to 24 wt.%. In general, the addition of silica to iron FT catalysts is known to improve the stability of the porous iron oxide/hydroxide network [2]. Silica enters the pores of the original network of the catalysts, thus providing a rigid matrix, which helps prevent a complete collapse of the pore structure of the catalyst. Although BET surface areas were found to be different for various catalysts, they do not appear to be directly related to the attrition resistance of the catalysts. After reduction with CO at 280°C for 16 h, the surface areas of the reduced catalysts were lower than that of the fresh catalysts. This may be due to the formation of carbonaceous deposits, which causes blocking of the pores of the catalyst [3]. The catalysts prepared had pore volumes in the 0.54–0.68 cm^3/g range and bulk

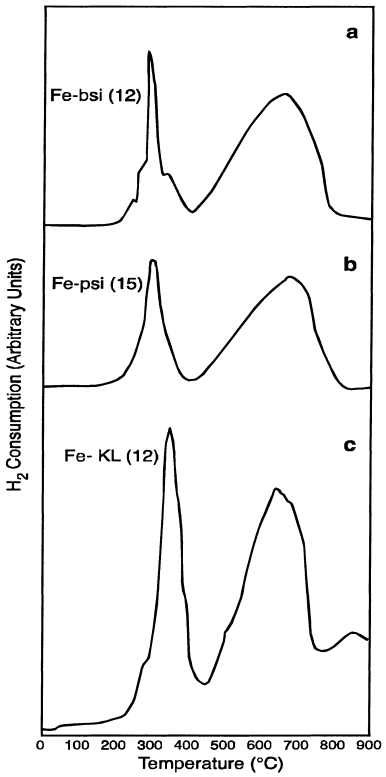

Fig. 3. TPR profile of: (a) Fe–bSi(12); (b) Fe–pSi(15); and (c) Fe–KL(12) catalysts.

densities in the 0.89–0.95 g/cm^3 range (not shown in Table 2). These densities are higher than typical precipitated catalysts, which have bulk densities of about 0.7 g/cm^3, and should allow easier separation from wax, which has a density of about 0.68 g/cm^3 [6].

The reduction behavior of the FT catalysts was studied by TPR. The profiles for binder silica, precipitated silica, and kaolin–clay catalysts are shown in Fig. 3. There were slight variations among the catalysts, with all showing peaks at 320 and 750°C. The peak at 320°C corresponds to the reduction $Fe_2O_3 \rightarrow Fe_3O_4$, and the peak at 750°C corresponds to the reduction of Fe_3O_4 to metallic iron. These curves are similar to others in the literature [2]. The small shoulder peak at roughly 250°C is due to the reduction CuO→Cu. A summary of the TPR characterization results for all the catalysts studied is given in Table 2. The TPR results indicate that hydrogen consumption during TPR decreased with an increase in the concentration of the silica content. However, this change was due mainly to decrease in the content of iron oxide in the catalysts, i.e., the hydrogen consumption was approximately the same for all catalysts when normalized by the iron content of each catalyst.

X-ray powder diffraction patterns of the fresh, CO-activated sample after activation, and after 100 h of FT synthesis for the binder and precipitated silica catalysts are shown in Figs. 4 and 5. The pattern has been plotted over 2θ value ranging from 5° to 75°. The pattern in Figs. 4 and 5 shows that the "fresh" samples are identical and are composed of α-Fe_2O_3. Other components, even the SiO_2 (binder silica and/or precipitated silica) were not detectable by XRD for any of these catalysts. The catalyst activated at 280°C with CO for 16 h exhibits peaks for Fe_3O_4 and χ-$Fe_{2.5}C$. The "used" sample contains mainly $Fe_{2.5}C$. The results are similar to those of Bukur et al. [2], who also observed χ-$Fe_{2.5}C$ after a similar reduction procedure.

The results of XRD analysis of kaolin binder containing iron catalyst samples are shown in Fig. 6. All five samples have two common features: a fairly large amorphous component, indicated by the high background maxima at 2θ about 35° and 62.5°, and the presence of what is best identified as $(Fe,Al)_3(Si,Al)_2O_5(OH)_4$. The presence of silicate indicates that the binder kaolinite that was added is not an inert component but rather that it reacted within the system to provide the Si, Al, and (OH). Note the similarity in the stoichiometry for kaolinite ($Al_2Si_2O_5(OH)_4$) and the above compound. The kaolinite seems to have incorporated some of the Fe. With so much Fe added to the original system, it seems that most of the iron added is contained in the amorphous phase.

The steady-state FT activity and selectivity results for the catalysts are shown in Table 3, along with data for Ruhrchemie catalyst for comparison. Following a short induction period, during which steady state was achieved, there was no significant change with time in CO conversions or hydrocarbon selectivities reported in Table 3 over the test duration, typically 80–125 h, for any of the catalysts. The α value for all catalysts tested range from 0.88 to 0.91. All catalysts tested were more active than Ruhrchemie, except the two with the highest kaolin content. The selectivity varied with silica type and content and kaolin

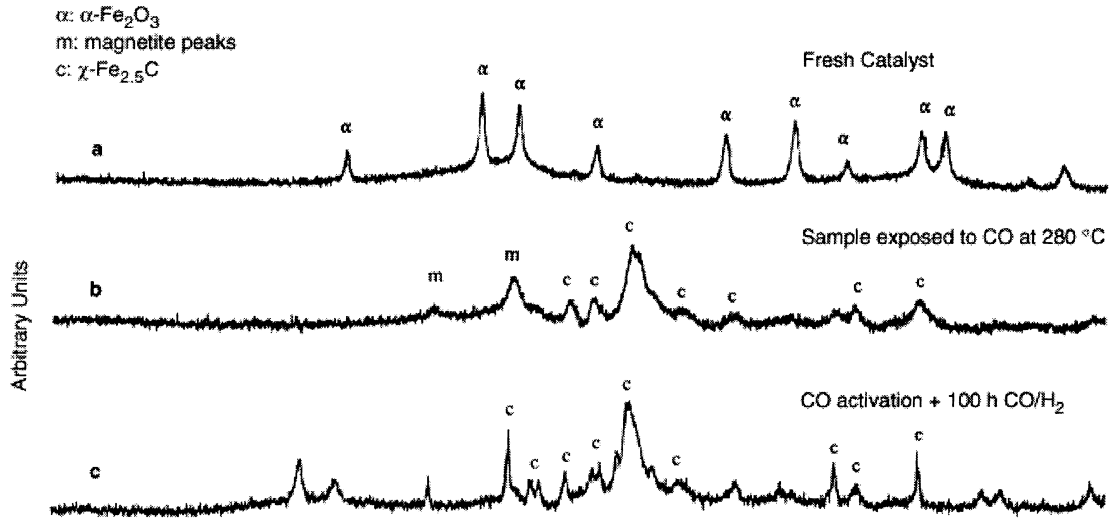

Fig. 4. XRD spectra of Fe–bSi(12) catalysts: (a) as-prepared fresh catalysts; (b) activiation in CO for 16 h at 280°C; and (c) activation in CO followed by FTS for 100 h at 270°C.

content. There was a beneficial effect of binder silica (up to 8–12 wt.%) on selectivity (lower methane and nearly constant C_5^+). However, as binder silica content increased above 12 wt.%, the C_1 and C_2 to C_4 selectivities increased at the expense of C_5^+ selectivity. As the precipitated silica content increased (at 12 wt.% binder silica), the selectivity to C_1 to C_{11} products increased. However, the C_5 to C_{11} selectivity for the catalysts containing precipitated silica was higher than the selectivity for those catalysts containing only binder silica. The activity/selectivity trends observed in the present study with the Ruhrchemie catalysts are generally in agreement with previous studies [3].

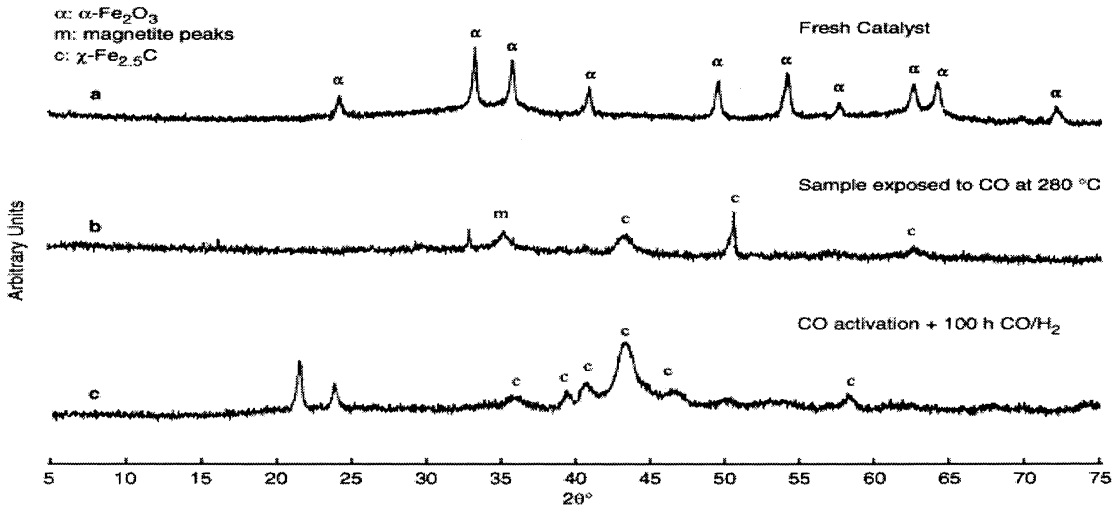

Fig. 5. XRD spectra of Fe–pSi(15) catalysts: (a) as-prepared fresh catalysts; (b) activation in CO for 16 h at 280°C; and (c) activation in CO followed by FTS for 100 h at 270°C.

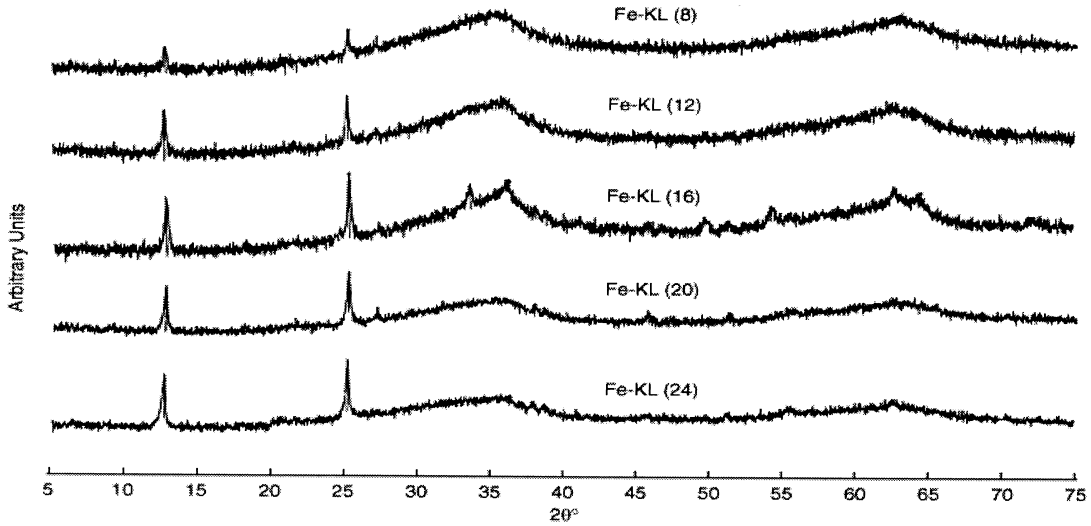

Fig. 6. XRD spectra of Fe–KL(*y*) iron catalysts.

Table 3
Catalyst activity and selectivity

Catalyst designation	CO conversion (%)[a]	Selectivity				α
		C_1	C_2–C_4	C_5–C_{11}	C_{12}^+	
Fe–bSi(4)	94.3	7.4	18.1	12.7	61.8	0.92
Fe–bSi(8)	94.1	6.8	17.6	13.0	62.5	0.91
Fe–bSi(12)	94.3	6.8	19.6	12.8	60.8	0.89
Fe–bSi(16)	95.5	9.9	25.0	17.3	47.8	0.87
Fe–bSi(20)	94.5	9.6	23.5	17.6	49.3	0.87
Fe–pSi(5)	95.5	8.8	23.2	22.0	46.0	0.87
Fe–pSi(10)	94.4	10.2	23.5	26.5	39.8	0.86
Fe–pSi(15)	90.1	10.2	22.4	30.5	36.9	0.87
Fe–pSi(20)	88.2	9.5	20.1	32.8	37.7	0.88
Fe–KL(8)	88.5	9.1	24.8	25.4	49.7	0.88
Fe–KL(12)	88.4	10.2	22.6	26.3	40.9	0.89
Fe–KL(16)	92.9	9.8	26.1	24.5	39.6	0.87
Fe–KL(20)	79.1	9.3	19.7	29.7	41.3	0.88
Fe–KL(24)	42.8	4.8	12.7	30.4	52.1	0.89
HPR-43	95.0	3.9	17.7	23.8	54.6	0.90
Ruhrchemie	86	8.3	21.3	14.3	56.1	0.90

[a] Measured at 270°C, 1.48 MPa, 2 NL/g-cat/h, $H_2/CO=0.67$.

Addition of kaolin binder to the catalyst containing 10 wt.% binder silica was detrimental to FT activity. CO conversion dropped from 94 to 42.8% as kaolin content increased from 0 to 24 wt.%. The methane selectivity also increased with kaolin content up to 12 wt.%. HPR-43 showed the lowest methane selectivity and nearly the highest CO conversion: 95% CO conversion over 125 h of testing at 270°C, 1.48 MPa, and 2 NL/g-cat/h with less than 4% methane selectivity. The attrition resistance of this catalysts was one of the highest among the catalysts tested.

4. Conclusion

The addition of binder silica to precipitated 100Fe/5Cu/4.2K FT catalyst followed by spray drying

increases the attrition resistance significantly. Within the range of the non-proprietary catalysts tested here, the optimum binder silica content is 10–12 wt.%. The FT activity and selectivity of this catalyst are better than a Ruhrchemie catalyst at 270°C and 1.48 MPa. The addition of precipitated silica or kaolin to catalyst containing 10–12 wt.% binder silica decreases attrition resistance and increases methane selectivity. A comparison of the attrition results shows that many of the spray dried iron catalysts in their calcined state are physically as strong as, or stronger than, the cobalt catalysts. These iron catalysts are therefore considered to have a strong potential for SBCR use.

Based on the experience gained, a new catalyst (HPR-43) has been successfully spray dried in 500 g quantity. This catalyst showed 95% CO conversion over 125 h of testing at 270°C, 1.48 MPa, and 2 NL/g-cat/h and had a less than 4% methane selectivity. Its attrition resistance was one of the highest among the catalysts tested.

Acknowledgements

The authors are grateful for US Department of Energy, Federal Energy Technology Center (FETC), University Coal Research (UCR) program for support of this research under grant numbers DE-FG22-96PC96217 and DE-PS26-98FT40108.

References

[1] Schulz, et al., Conference on Natural Gas II, Elsevier, Amsterdam, Surf. Sci. Ser. 81 (1994) 455.
[2] D.B. Bukur, K. Okabe, M.P. Rosynek, C. Li, D. Wang, K.R.P.M. Rao, G.P. Huffman, J. Catal. 155 (1995) 353.
[3] D.B. Bukur, L. Nowicki, R.K. Manne, X. Lang, J. Catal. 155 (1995) 366.
[4] A. Raje, J.R. Inga, B.H. Davis, Fuel 76 (1997) 273.
[5] D. Stern, A.T. Bell, H. Heinemann, Ind. Eng. Chem. Process. Des. Dev. 24 (1985) 213.
[6] T.J. Donnelly, C.N. Satterfield, Appl. Catal. 56 (1989) 231.
[7] B.L. Bhatt, E.C. Heydorn, P.J.A. Tijm, Proceedings of the 1997 Coal Liquefaction and Solid Fuels Contractors Review Conference, Vol. 3/4, US Department of Energy, Federal Energy Technology Center, Pittsburgh, PA, September 1999, p. 41.
[8] D.S. Kalakkad, M.D. Shroff, S. Kohler, N.B. Jackson, A.K. Datye, Appl. Catal. A 133 (1995) 335.
[9] M.D. Shroff, D.S. Kalakkad, K.E. Coulter, S.D. Kohler, M.S. Harrington, N.B. Jackson, A.G. Sault, A.K. Datye, J. Catal. 156 (1995) 185.
[10] R. Zhao, J.G. Goodwin Jr., R. Oukaci, Appl. Catal. A 189 (1999) 99.
[11] B.D. Bukur, D. Mukesh, S.A. Patel, Ind. Eng. Chem. Res. 29 (1990) 194.
[12] E.J. Demmel, US Patent 5288739 (1994).
[13] A.K. Datye, Study Surf. Sci. Catal. 101 (1996) 1421.